JVSTB Journal of Vacuum Science & Technology B

Experimental verification of achieving vertical sidewalls for nanoscale features in electron-beam lithography

Soo-Young Lee, Jin Choi, Sang-Hee Lee, In-Kyun Shin, Chan-Uk Jeon, and Sang-Chul Jeon

Citation: Journal of Vacuum Science & Technology B **32**, 06F510 (2014); doi: 10.1116/1.4901171
View online: http://dx.doi.org/10.1116/1.4901171
View Table of Contents: http://scitation.aip.org/content/avs/journal/jvstb/32/6?ver=pdfcov
Published by the AVS: Science & Technology of Materials, Interfaces, and Processing

Experimental verification of achieving vertical sidewalls for nanoscale features in electron-beam lithography

Soo-Young Lee[a)]
Department of Electrical and Computer Engineering, Auburn University, Auburn, Alabama 36849

Jin Choi, Sang-Hee Lee, In-Kyun Shin, and Chan-Uk Jeon
Samsung Electronics, Mask Development Team, Hwasung, Kyunggi-Do 445-701, South Korea

Sang-Chul Jeon
National NanoFab Center, Yuseong-Gu, Daejeon 305-806, South Korea

(Received 27 June 2014; accepted 27 October 2014; published 11 November 2014)

It is often necessary to achieve a vertical sidewall in the remaining resist profile obtained through electron-beam lithographic process. For nanoscale features, the spatial dose distribution of V-shape typically used in a conventional two-dimensional proximity effect correction scheme cannot easily achieve a vertical sidewall while also minimizing the critical dimension (CD) error. In an earlier study, it was shown through simulation based on a three-dimensional model that new types of spatial dose distributions, i.e., M- and A-shapes, are effective in achieving vertical sidewalls and minimizing the CD error and total dose. These two dose distributions exploit the fact that the exposure varies along the depth dimension with high and low contrasts at the top and bottom layers of resist, respectively. In this study, a number of experiments have been carried out in order to verify the simulation results reported earlier. This paper includes a review of the new dose distribution types and experimental results with a detailed discussion. © *2014 American Vacuum Society*.
[http://dx.doi.org/10.1116/1.4901171]

I. INTRODUCTION

In electron-beam (e-beam) lithography, electron scattering in the resist layer leads to the proximity effect, which can make the written pattern significantly different from the target one. Many researchers have worked on correcting the proximity effect and various correction schemes have been developed.[1–9] Most of the schemes are based on a two-dimensional (2D) model of resist and therefore do not consider the resist depth dimension during correction. Any variation of feature size, such as line width, along the resist depth dimension is not considered. Or equivalently, the feature size averaged along the depth dimension is employed in the correction. A 2D correction may be acceptable for large features since such a variation can be negligible compared to the feature size. However, for nanoscale features, the variation becomes relatively significant such that it cannot be ignored. Therefore, a three-dimensional (3D) model of the resist layer must be employed to take into account the variation of resist profile along the resist depth dimension. In an earlier study, the 3D proximity effect was analyzed in detail.[10]

A true 3D correction method has been introduced to minimize the critical dimension (CD) error in each layer of resist.[11,12] In this correction procedure, the remaining resist profile is obtained through simulation and the spatial dose distribution is adjusted to reduce the maximum CD error among resist layers. Since the resist profile, instead of the exposure (energy deposited in the resist) distribution, is checked during the correction, the correction result must be more realistic. Note that this task of reducing the CD error on each layer as much as possible may be reformulated as minimizing the average CD error with a vertical sidewall in the resist profile. Recently, the issue of achieving a vertical sidewall while minimizing the CD error for nanoscale features was considered through an extensive simulation.[13] It has been shown that employing a 3D model allows one to find a spatial dose distribution which minimizes the maximum CD error and achieves a vertical sidewall. An even more important finding from the study is that the conventional shape of spatial dose distribution, "V-shape" (where the dose is higher toward the edge of feature), often obtained by a 2D proximity effect correction method, is not always optimal for nanoscale features. Two new types of dose distributions, i.e., "M-shape" and "A-shape," are shown to be more effective than the V-shape distribution in achieving vertical sidewall and minimizing the maximum CD error with a lower total dose required.

In this study, the simulation results obtained in the previous work[13] have been verified through experiment, and the experimental results are presented in this paper. Line features are exposed using the different types of dose distribution and the cross-section SEM images of the remaining resist profiles are examined in comparing the new types of dose distributions with the conventional types under the same conditions. Also, different resist types are considered to observe the performance trend of the new types of dose distributions. It has been shown that the experimental results match well with the simulation results.

The rest of the paper is organized as follows. The simulation study and the results are briefly reviewed in Sec. II. The experimental procedure is described in Sec. III. The results from experiment are provided with detailed discussion in Sec. IV. Finally, a summary is given in Sec. V.

[a)]Electronic mail: leesooy@eng.auburn.edu

II. SIMULATION STUDY

In this section, the simulation study on achieving a vertical sidewall in the remaining resist profile is reviewed.[13] The main objective of this research is to realize a vertical sidewall in the resist profile while minimizing the CD errors in all layers of resist and the total dose, based on a 3D model of the substrate system. The 3D exposure distribution in the resist is computed and then converted into the developing rate. From the distribution of the developing rate, the remaining resist profile is obtained through development simulation. The spatial dose distribution is optimized such that the resist profile is as close to the target profile as possible.

A. Resist profile

A typical substrate system is illustrated in Fig. 1, where the X-Y plane corresponds to the top surface of resist and the resist depth is along the Z-dimension. The 3D point spread function (PSF) is denoted by $psf(x,y,z)$, which describes the spatial distribution of the exposure in the resist when a point on the X-Y plane is exposed. Note that the PSF, $psf(x,y,z)$, reflects all of the phenomena affecting energy deposition in the resist, including the e-beam blur. The e-beam dose given to the point $(x,y,0)$ on the surface of the resist for writing a circuit feature or pattern may be denoted by $d(x,y,0)$. Then, the 3D spatial distribution of the exposure in the resist, $e(x,y,z)$, can be computed layer by layer through convolution as

$$e(x,y,z) = \int\int d(x-x',y-y',0)psf(x',y',z)dx'dy'. \quad (1)$$

The resist developing rate is not linearly proportional to the exposure.[14] Therefore, the exposure is converted into the developing rate through a nonlinear exposure-to-rate conversion formula, which can be derived experimentally. The remaining resist profile is estimated from the 3D distribution of the developing rate through the development simulation, which is carried out by the newly developed fast method for resist development simulation.[15] It has been shown that resist profiles obtained by the new method are very close to those by the cell-removal and fast-marching methods.

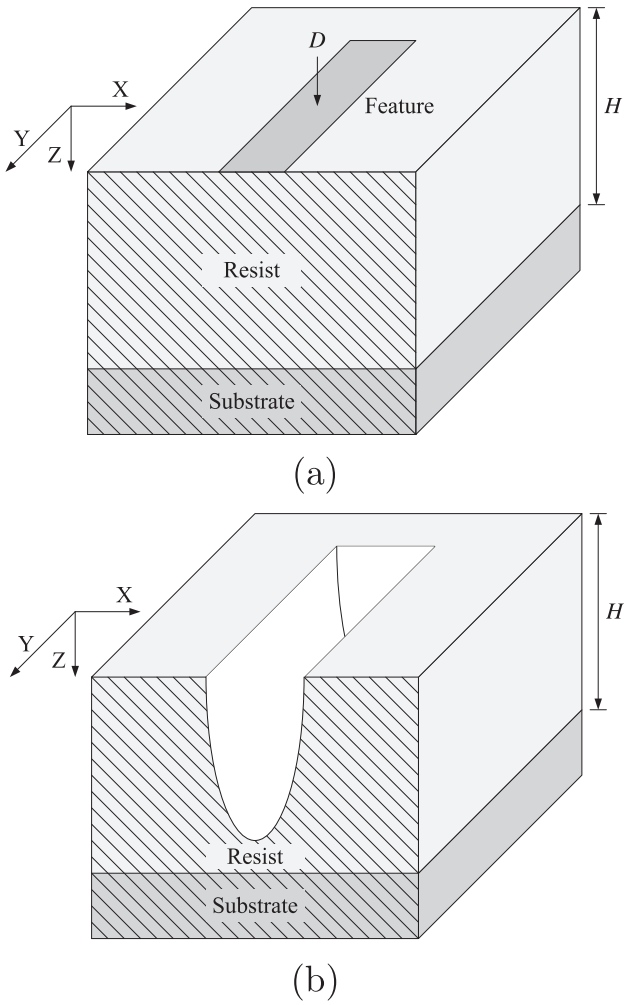

FIG. 1. Illustration of (a) the substrate system, where H is the initial thickness of the resist and D is the dose given to the feature, and (b) the final remaining resist profile after the development process.

B. New types of dose distribution

A conventional approach to the 2D proximity effect correction is to achieve a uniform exposure within a feature, which is well above the developing threshold while achieving a low exposure outside the feature. This approach usually leads to a dose distribution, which is high at the edge of a feature and decreases toward the center, i.e., a dose distribution that is a V-shape, referred to as type-V [see Fig. 2(a)]. This is a reasonable dose distribution for large features, but for nanoscale features where the width variation along the resist depth dimension in the resist profile can be relatively significant compared to the feature size (width), a dose distribution of type-V may not be optimal in terms of minimizing CD errors at all layers (of resist) and the total dose. Such a dose distribution tends to lead to a resist profile of overcut, i.e., wider at an upper layer. A higher dose is given to a point closer to the feature edge and therefore the resist is developed faster at the edge than at the center, leading to a larger width at an upper layer.

It has been shown through an extensive simulation that new types of dose distributions, namely, type-M [the dose distribution of M-shape: Fig. 2(b)] and type-A [the dose distribution of A-shape: Fig. 2(c)], are significantly more effective in achieving a vertical sidewall of resist profile than type-V for nanoscale features. The effectiveness of the type-M and type-A dose distributions in achieving a vertical sidewall stems from their resulting 3D distributions of exposure. Our previous work[16] has shown that the distribution of exposure along the depth dimension behaves quite differently between the exposed area and the unexposed area. In the exposed area, the exposure usually decreases along the depth dimension, while in the unexposed area, the exposure increases from the top to bottom layer since the forward scattering is reduced greatly and the relative level of backscattering is increased. The type-M and type-A dose distributions exploit this behavior of 3D exposure distribution in the resist.

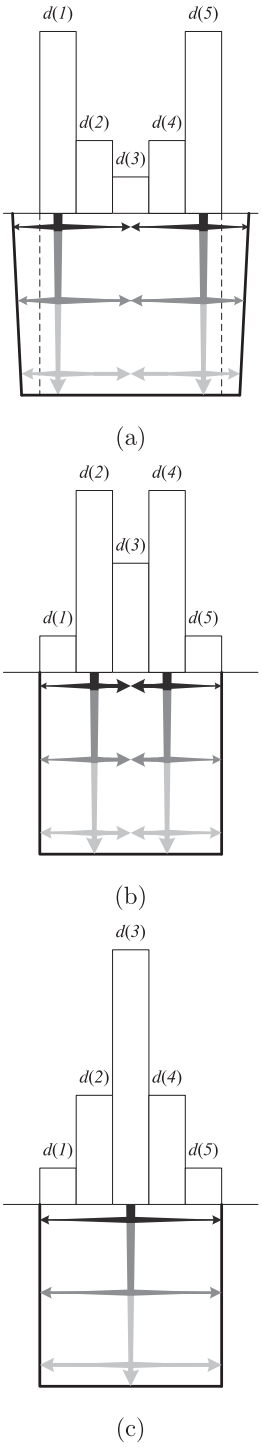

FIG. 2. Dose distribution types: (a) type-V, (b) type-M, and (c) type-A. In each type, the dominant developing paths are illustrated where the intensity and width of a path indicate the development stage and the relative developing rate, respectively. The darker the intensity is, the earlier the stage of development; and the narrower the width is, the lower the developing rate.

C. Optimization and results

Given a type of dose distribution, the optimal spatial distribution of dose is derived (for detail, refer to our previous work[13]). The feature (e.g., line) is partitioned into five regions along the length dimension (see Fig. 3) and the dose for each region [$d(i)$: dose for region i, where $i = 1, \ldots, 5$] is

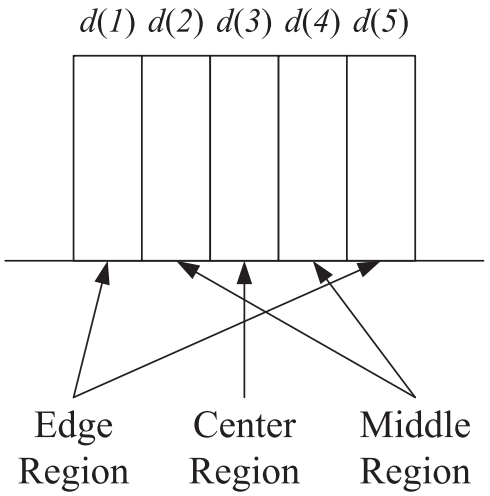

FIG. 3. Region-wise feature partitioning is illustrated for a uniform dose distribution.

determined through an iterative procedure such that the deviation from the target resist profile, i.e., vertical sidewall, is minimized. In each iteration, the remaining resist profile is obtained by the resist development simulation, and the CD error (width error) in each layer (top, middle, and bottom) of resist is computed (see Fig. 4). Then, the dose of each region is adjusted to reduce the maximum CD error among the layers. Minimization of the total (equivalently average) dose required is also incorporated into this optimization procedure. The total (or equivalently average) dose is defined as $\frac{1}{5}\sum_{i=1}^{5} d(i)$ (refer to Fig. 3).

A typical set of simulation results is provided in Fig. 5 where the total (average) dose is 250 μC/cm^2 for all types of dose distributions. The sidewalls achieved by the type-M and type-A dose distributions are nearly vertical whereas the line is not fully developed or an overcut is obtained in the cases of the uniform and type-V dose distributions. Also, the total dose required for achieving an equivalent vertical sidewall with full development is shown to be lower for the

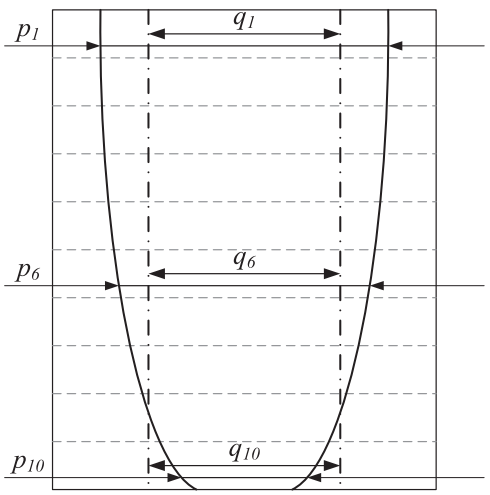

FIG. 4. Cross-section of the resist profile is illustrated for a line feature where p_j and q_j are the actual and target widths at the jth layer, respectively, and the resist is modeled by ten layers.

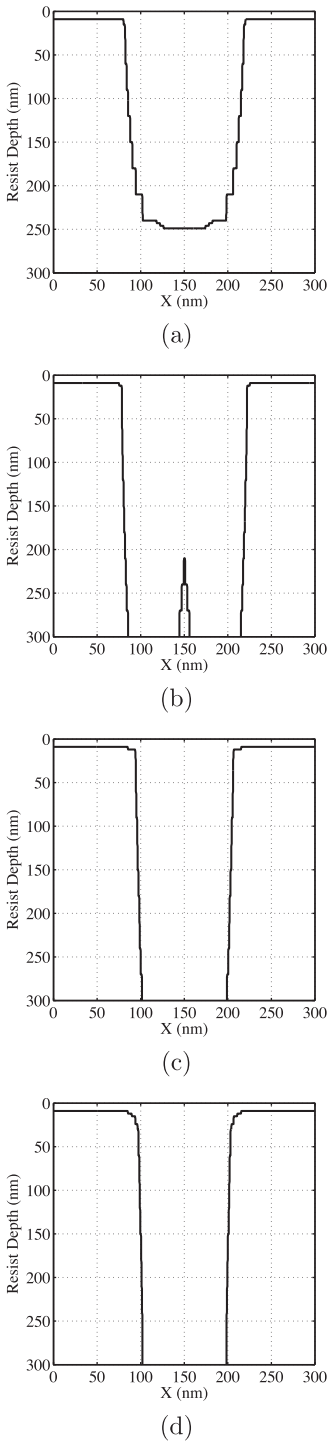

FIG. 5. Simulated cross-section resist profiles: (a) the uniform, (b) type-V dose, (c) type-M dose, and (d) type-A dose distributions on a substrate system of 300 nm PMMA on Si (total dose 250 μC/cm^2).

type-M and type-A distributions than for the uniform and type-V dose distributions.

III. EXPERIMENT

In order to verify the results from the simulation study described in Sec. II., experiments have been carried out with a line feature. The line width is 100 nm and the line length is much longer than the full scattering range of electrons. The substrate system is composed of a resist on Si. Two different resist types, poly(methyl methacrylate) (PMMA) and ZEP, are used with a thickness of 300 nm. After the resist development process, the cross-sections of the remaining resist profiles obtained by different types of dose distributions are compared. The experimental procedures are described below.

The wafer was coated with ZEP 520A (ZEON) or PMMA (AR-P 671.09, 950 K 9% in Chlorobenzene). The e-beam writing was carried out on the ELIONIX ELS7000 with an acceleration voltage of 50 keV, a beam current of 100 pA, a beam diameter of 2 nm, and a beam interval of 10 nm. The sample was developed for 40 s in methyl isobutyl ketone: isopropyl alcohol (MIBK:IPA) = 1:2 in the case of PMMA and for 20 s in o-xylene in the case of ZEP. The developed sample was subsequently coated with 10 nm of Pt for imaging. The cross-section of the remaining resist profile was imaged using a field emission scanning electron microscope (FE-SEM), Hitachi S-4800.

IV. RESULTS AND DISCUSSION

In Fig. 6, the results (cross-section SEM images of remaining resist profiles) for the PMMA of 300 nm are provided where the total dose is 290 μC/cm^2 for all of the uniform, type-V and type-M dose distributions. When the line is exposed with the uniform dose, i.e., no control of spatial dose distribution, it is not fully developed resulting in an overcut of the resist profile. It should be also noted that the line width at the top layer is much larger than the target width of 100 nm. The resist profile obtained by the type-V dose distribution is similar with that by the uniform dose, i.e., not fully developed and overcut. When the doses for the edge regions are made higher (with a lower dose for the center region to maintain the same total dose), the line gets developed less overall, with the resist profile showing two shallow valleys corresponding to the two edge regions. However, the type-M dose distribution is able to achieve a resist profile very close to the target profile, i.e., fully developed with a vertical sidewall. Nevertheless, it needs to be pointed out that the line width is a little wider than 100 nm, which indicates that the total dose can be reduced.

In Fig. 7, the type-M and type-A dose distributions are compared when the total dose is lowered to 275 μC/cm^2. Due to the reduced dose level, the type-M dose distribution is not able to fully develop the line, which leads to an overcut of the resist profile. On the other hand, the resist profile obtained by the type-A dose distribution is closest to the target profile in terms of line width (CD error) and sidewall shape. It is clear that type-A not only achieves the target profile with the minimal CD error but also lowers the total dose required.

A different resist, ZEP, is also employed in verifying the simulation results. In Fig. 8, the results for the resist thickness of 300 nm are shown for the uniform, type-V, type-M, and type-A dose distributions. The total dose is 187 μC/cm^2 for all types. In this figure, a much larger difference between the conventional types (uniform and type-V) and the new

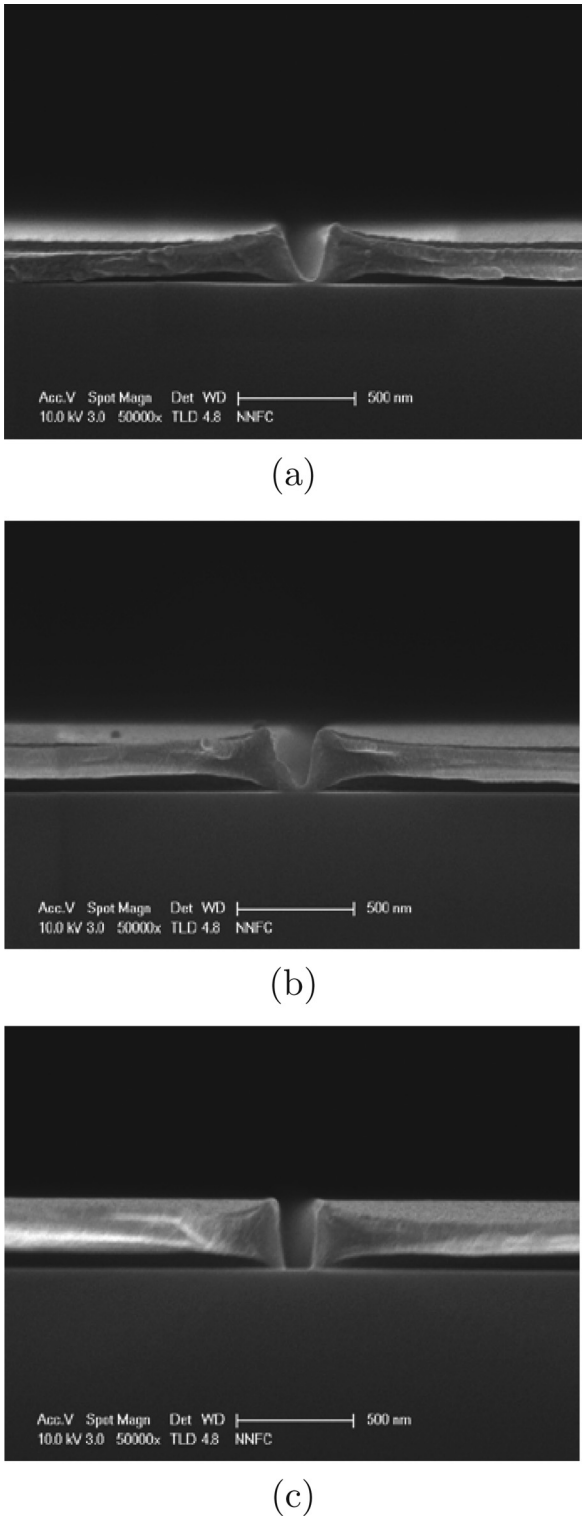

FIG. 6. Cross-section SEM images of resist profiles on 300 nm PMMA on Si with a total dose of 290 μC/cm^2: (a) uniform, (b) type-V with $\{d(i)\} = \{424, 232, 138, 232, 424\}$, and (c) type-M with $\{d(i)\} = \{90, 615, 40, 615, 90\}$.

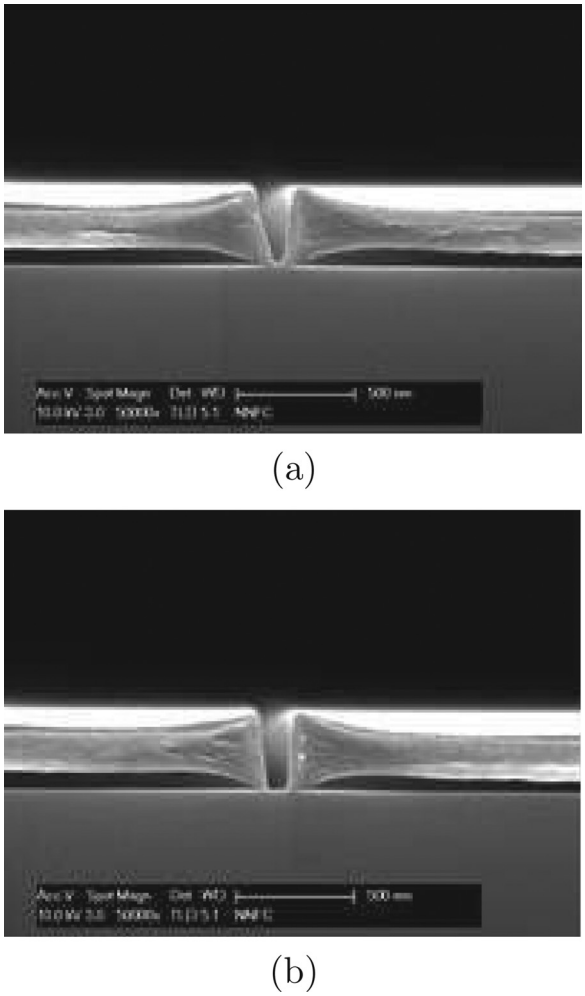

FIG. 7. Cross-section SEM images of resist profiles on 300 nm PMMA on Si with a total dose of 275 μC/cm^2: (a) type-M with $\{d(i)\} = \{30, 620, 75, 620, 30\}$, and (b) type-A with $\{d(i)\} = \{31, 254, 805, 254, 31\}$.

types (type-M and type-A) of dose distributions can be seen. For the uniform dose distribution, the line is only partially developed with the maximum depth (which is at the center of the line) barely reaching one third of the resist thickness. The resist profile obtained by the type-V dose distribution is not much different from that by the uniform dose distribution, which is severely under-developed. When the type-M dose distribution is used, the line is almost fully developed. Though a slight under-development toward the edges of line makes the overall profile rounded at the bottom layer of the resist, the resist profile is much improved and closer to the target profile than those by the uniform and type-V dose distributions. A significant improvement by the type-A dose distribution compared to the type-M dose distribution is clearly visible in Fig. 8(d). The resist profile obtained by type-A is almost the same as the target profile, i.e., the sidewall is vertical and the line width is very close to 100 nm at all layers.

All of the results in each set (figure) are obtained under the same experimental conditions, including the total dose and developing time. That is, the four types of dose distributions are compared under the same conditions and therefore the difference among their resist profiles is only due to the different spatial dose distributions, i.e., different spatial distributions of the same total dose. If, for example, the total dose is increased for the uniform and type-V dose distributions, the feature

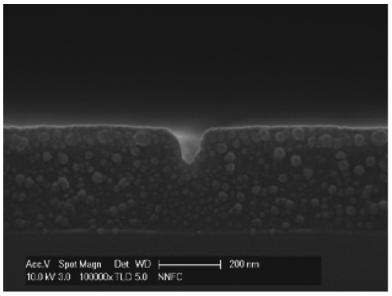
(a)

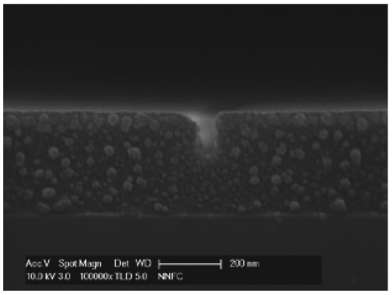
(b)

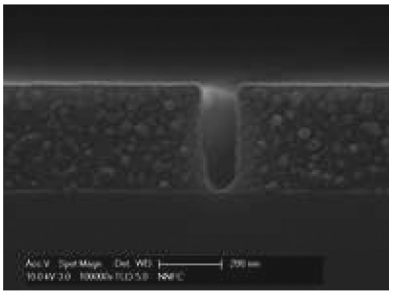
(c)

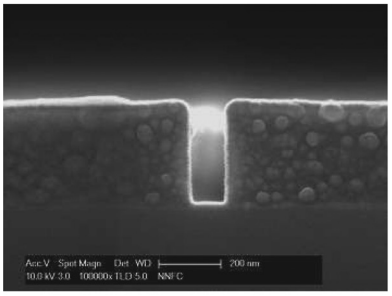
(d)

FIG. 8. Cross-section SEM images of resist profiles on 300 nm ZEP on Si with a total dose of 187 μC/cm^2: (a) uniform, (b) type-V with $\{d(i)\} = \{234, 187, 93, 187, 234\}$, (c) type-M with $\{d(i)\} = \{47, 374, 93, 374, 47\}$, and (d) type-A with $\{d(i)\} = \{42, 168, 515, 168, 42\}$.

would be further developed, being eventually fully developed, though their resist profiles are likely to be of over-size and possibly overcut depending on the resist thickness and feature size.

While the new types of dose distributions control the spatial distribution of dose, they also include the ability of shape adjustment, e.g., shrinking the feature area to be exposed. When the dose in the edge region is zero or very low and the doses in the other regions are similar, the resulting dose distribution is equivalent to that where the feature area to be exposed is reduced with a uniform dose. It should be noted that the effect achieved by the type-A dose distribution is similar to that by some of the proximity effect correction methods, such as the "undersize-overdose" method[17] and the shape correction method.[18] These methods have the advantage that the number of feature shapes to be processed is smaller since they do not partition each feature. This would be beneficial, particularly on a shaped-beam machine. On the other hand, the type-A dose distribution offers the ability to further optimize the resist profile. It would be worthwhile to compare the new types of dose distributions with the shape adjustment approaches (e.g., the undersize-overdose method), which is one of our current research activities.

V. SUMMARY

In an earlier study, the issue of achieving a target sidewall shape (vertical sidewall) in the resist profile while minimizing the CD error and total dose in e-beam lithography was investigated. It was suggested that the conventional types (uniform and type-V) of dose distributions, obtained by a 2D proximity effect correction scheme, may not be optimal for nanoscale features. Through an extensive simulation, it has been shown that the new types (type-M and type-A) of dose distributions are more effective in realizing a vertical sidewall of nanoscale feature with the CD error and total dose minimized. In this study, the simulation results have been verified through experiment. It is observed in the experimental results that the sidewalls obtained by type-A and type-M dose distributions are more vertical than those by the uniform and type-V dose distributions. Also, the CD error at each layer of resist is smaller for type-M and type-A, and the minimum total dose required for the full development of a feature and the minimum possible CD error is lower for type-M and type-A. In addition, the type-A dose distribution performs better than the type-M dose distribution, especially when the aspect ratio (the ratio of resist thickness to line width) is relatively large. Therefore, the method of achieving a target resist profile for nanoscale features using the new types of dose distributions (type-M and type-A), proposed through simulation in an earlier study and verified experimentally in this study, has a good potential to be effective in practice. A drawback of the new types is that the number of feature shapes to be processed by an e-beam system is increased.

ACKNOWLEDGMENT

This work was supported by a research grant from Samsung Electronics Co., Ltd.

[1]R. Rau, J. McClellan, and T. Drabik, J. Vac. Sci. Technol., B **14**, 2445 (1996).
[2]G. P. Watson, L. A. Fetter, and J. A. Liddle, J. Vac. Sci. Technol., B **15**, 2309 (1997).
[3]G. P. Watson, S. D. Berger, and J. A. Liddle, J. Vac. Sci. Technol., B **16**, 3256 (1998).
[4]S.-Y. Lee and B. D. Cook, IEEE Trans. Semicond. Manuf. **11**, 108 (1998).
[5]C. S. Ea and A. D. Brown, J. Vac. Sci. Technol., B **17**, 323 (1999).
[6]U. Hofmann, R. Crandall, and L. Johnson, J. Vac. Sci. Technol., B **17**, 2940 (1999).

[7]K. Takahashi, M. Osawa, M. Sato, H. Arimoto, K. Ogino, H. Hoshino, and Y. Machida, J. Vac. Sci. Technol., B **18**, 3150 (2000).
[8]C. S. Ea and A. D. Brown, J. Vac. Sci. Technol., B **19**, 1985 (2001).
[9]M. Osawa, K. Takahashi, M. Sato, H. Arimoto, K. Ogino, H. Hoshino, and Y. Machida, J. Vac. Sci. Technol., B **19**, 2483 (2001).
[10]S.-Y. Lee and K. Anbumony, Microelectron. Eng. **83**, 336 (2006).
[11]K. Anbumony and S.-Y. Lee, J. Vac. Sci. Technol., B **24**, 3115 (2006).
[12]Q. Dai, S.-Y. Lee, S.-H. Lee, B.-G. Kim, and H.-K. Cho, J. Vac. Sci. Technol., B **29**, 06F314 (2011).
[13]Q. Dai, S.-Y. Lee, S.-H. Lee, B.-G. Kim, and H.-K. Cho, J. Vac. Sci. Technol., B **30**, 06F307 (2012).
[14]J. Kim, D. C. Joy, and S.-Y. Lee, Microelectron. Eng. **84**, 2859 (2007).
[15]Q. Dai, R. Guo, S.-Y. Lee, J. Choi, S.-H. Lee, I.-K. Shin, C.-W. Jeon, B.-G. Kim, and H.-K. Cho, Microelectron. Eng. **127**, 86 (2014).
[16]Q. Dai, S.-Y. Lee, S.-H. Lee, B.-G. Kim, and H.-K. Cho, Microelectron. Eng. **88**, 902 (2011).
[17]V. Guzenko, B. Pedrini, A. Menzel, and C. David, Microelectron. Eng. **121**, 127 (2014).
[18]B. D. Cook and S.-Y. Lee, IEEE Trans. Semicond. Manuf. **11**, 117 (1998).